John von Neumann Institute for Computing

Lyapunov Instabilities of Extended Systems

H. Yang, G. Radons

published in

NIC Symposium 2008,
G. Münster, D. Wolf, M. Kremer (Editors),
John von Neumann Institute for Computing, Jülich,
NIC Series, Vol. **39**, ISBN 978-3-9810843-5-1, pp. 349-358, 2008.

http://www.fz-juelich.de/nic-series/volume39

Lyapunov Instabilities of Extended Systems

Hong-liu Yang and Günter Radons

Institute of Physics, Chemnitz University of Technology, D-09107 Chemnitz, Germany
E-mail: {hongliu.yang, radons}@physik.tu-chemnitz.de

Here we review our current results on Lyapunov spectra and Lyapunov vectors (LVs) of various extended systems with continuous symmetries. The major part of the article is devoted to the study of Lennard-Jones fluids in one- and two-dimensional spaces. By using the newly introduced LV correlation functions, we demonstrate that the LVs with $\lambda \approx 0$ are highly dominated by a few components with low wave numbers, which implies the existence of hydrodynamic Lyapunov modes in soft-potential systems. Despite the wave-like character of the LVs, no step-like structure exists in the Lyapunov spectrum of the systems studied here, in contrast to the hard-core case. Studies on dynamical LV structure factors conclude that HLMs in Lennard-Jones fluids are propagating. We also briefly outline our current results on the universal features of HLMs in a class of spatially extended systems with continuous symmetries. HLMs in Hamiltonian and dissipative systems are found to differ both in respect of spatial structure and in the dynamical evolution.

1 Introduction

One of the most successful theories in modern science is statistical mechanics, which allows us to understand the macroscopic (thermodynamic) properties of matter from a statistical analysis of the microscopic (mechanical) behaviour of the constituent particles. In spite of this, using certain probabilistic assumptions such as Boltzmann's *Stosszahlansatz* causes the lack of a firm foundation of this theory, especially for non-equilibrium statistical mechanics. Fortunately, the concept of chaotic dynamics developed in the 20th century is a good candidate for accounting for these difficulties. Instead of the probabilistic assumptions, the dynamical instability of trajectories can make available the necessary fast loss of time correlations, ergodicity, mixing and other dynamical randomness. It is generally expected that dynamical instability is at the basis of macroscopic transport phenomena and that one can find certain connections between them. Some beautiful theories in this direction were already developed in the past decade[1], where the Lyapunov exponents were related to certain transport coefficients.

Very recently, molecular dynamics simulations on hard-core systems revealed the existence of regular collective perturbations corresponding to the smallest positive Lyapunov exponents (LEs), named hydrodynamic Lyapunov modes[2]. This provides a new possibility for the connection between Lyapunov vectors, a quantity characterizing the dynamical instability of trajectories, and macroscopic transport properties. A lot of work[3–8] has been done to identify this phenomenon and to find out its origin. The appearance of these modes is commonly thought to be due to the conservation of certain quantities in the systems studied[3–7]. A natural consequence of this expectation is that the appearance of such modes might not be an exclusive feature of hard-core systems and might be generic to a large class of Hamiltonian systems. However, until very recently, these modes have only been identified in the computer simulations of hard-core systems[3,8].

In this article, we give an overview of our recent results on Lyapunov instabilities of various extended systems with continuous symmetries, especially on the identification

and characterization of hydrodynamic Lyapunov modes. The major part of the article is devoted to the investigation of Lennard-Jones fluids, wherein the HLMs are, for the first time, identified in systems with soft-potential interactions[9,10]. Our new technique, based on a spectral analysis of LVs, shows strong evidence that hydrodynamic Lyapunov modes do exist in these cases. In section 6, we will go beyond the many-particle systems and show some universal features of HLMs in a large class of extended systems. Details of these investigations can be found in our publications[11–13].

2 Numerical Method for Determining Lyapunov Exponents and Vectors

2.1 Standard Method

The equations of motion for a many-body system may always be written as a set of first order differential equations $\dot{\Gamma}(t) = F(\Gamma(t))$, where Γ is a vector in the D-dimensional phase space. The tangent space dynamics describing infinitesimal perturbations around a reference trajectory $\Gamma(t)$ is given by

$$\delta\dot{\Gamma} = M(\Gamma(t)) \cdot \delta\Gamma \tag{1}$$

with the Jacobian $M = \frac{dF}{d\Gamma}$. The time averaged expansion or contraction rates of $\delta\Gamma(t)$ are given by the Lyapunov exponents. For a $D-$dimensional dynamical system there exist in total D Lyapunov exponents for D different directions in tangent space. The orientation vectors of these directions are the Lyapunov vectors $e^{(\alpha)}(t)$, $\alpha = 1,\cdots,D$.

For the calculation of the Lyapunov exponents and vectors the offset vectors have to be reorthogonalized periodically, either by means of Gram-Schmidt orthogonalization or QR decomposition[14]. To obtain scientifically useful results, one needs large particle numbers and long integration times for the calculation of certain long time averages. This enforces the use of parallel implementations of the corresponding algorithms. It turns out that the repeated reorthogonalization is the most time consuming part of the algorithm.

2.2 Parallel Realization

As parallel reorthogonalization procedures we have realized and tested several parallel versions of Gram-Schmidt orthogonalization and of QR factorization based on blockwise Householder reflection. The parallel version of classical Gram-Schmidt (CGS) orthogonalization is enriched by a reorthogonalization test which avoids a loss of orthogonality by dynamically using iterated CGS. All parallel procedures are based on a 2-dimensional logical processor grid and a corresponding block-cyclic data distribution of the matrix of offset vectors. Row-cyclic and column-cyclic distributions are included due to parameterized block sizes, which can be chosen appropriately. Special care was also taken to offer a modular structure and the possibility for including efficient sequential basic operations, such as those from BLAS, in order to efficiently exploit the processor or node architecture.

Performance tests of parallel algorithms have been done on a Beowulf cluster, a cluster of dual Xeon nodes, and an IBM Regatta p690+. Results can be found in[15].

3 Correlation Functions for Lyapunov Vectors

In the spirit of molecular hydrodynamics[16], we introduced in[9,10] a dynamical variable called *LV fluctuation density*,

$$u^{(\alpha)}(r,t) = \sum_{j=1}^{N} \delta x_j^{(\alpha)}(t) \cdot \delta(r - r_j(t)), \tag{2}$$

where $\delta(z)$ is Dirac's delta function, $r_j(t)$ is the position coordinate of the j-th particle, and $\{\delta x_j^{(\alpha)}(t)\}$ is the coordinate part of the α-th Lyapunov vector at time t. The spatial structure of LVs is characterized by the *static LV structure factor* defined as

$$S_u^{(\alpha\alpha)}(k) = \int \langle u^{(\alpha)}(r,0) u^{(\alpha)}(0,0) \rangle e^{-jk\cdot r} dr, \tag{3}$$

which is simply the spatial power spectrum of the LV fluctuation density. Information on the dynamics of LVs can be extracted via the *dynamic LV structure factor*, which is defined as

$$S_u^{(\alpha\alpha)}(k,\omega) = \int\int \langle u^{(\alpha)}(r,t) u^{(\alpha)}(0,0) \rangle e^{-jk\cdot r} e^{j\omega t} dr dt. \tag{4}$$

With the help of these quantities the controversy[2,3] about the existence of hydrodynamic Lyapunov modes in soft-potential systems has been successfully resolved[9].

4 Numerical Results for 1d Lennard-Jones Fluids

4.1 Models

The Lennard-Jones system studied has the Hamiltonian $H = \sum_{j=1}^{N} mv_i^2/2 + \sum_{j<l} V(x_l - x_j)$. where the interaction potential among particles is $V(r) = 4\epsilon\left[(\frac{\sigma}{r})^{12} - (\frac{\sigma}{r})^{6}\right] - V_c$ if $r \leq r_c$ and $V(r) = 0$ otherwise with $V_c = 4\epsilon\left[(\frac{\sigma}{r_c})^{12} - (\frac{\sigma}{r_c})^{6}\right]$. Here the potential is truncated in order to lower the computational burden.

The system is integrated using the velocity form of the Verlet algorithm with periodic boundary conditions. The standard method invented by Benettin et al. and Shimada and Nagashima[14] is used to calculate the Lyapunov characteristics of the systems studied. Other technical details can be found in Ref.[9]. Throughout this paper, the particle number is typically denoted by N, the length of the system by L and the temperature by T.

4.2 Smooth Lyapunov Spectrum with Strong Short-Time Fluctuations

The Lyapunov spectrum for the case $N = 100$, $L = 1000$ and $T = 0.2$ is shown in Fig. 1. Only half of the spectrum is shown here, since all LEs of Hamiltonian systems come in pairs according to the conjugate-pairing rule. In the enlargement shown in the inset of Fig. 1 for the part near $\lambda^{(\alpha)} \approx 0$, one can not see any step-wise structure in the Lyapunov spectrum, in contrast to the case of hard-core systems[3]. This is the typical result obtained for our soft potential system.

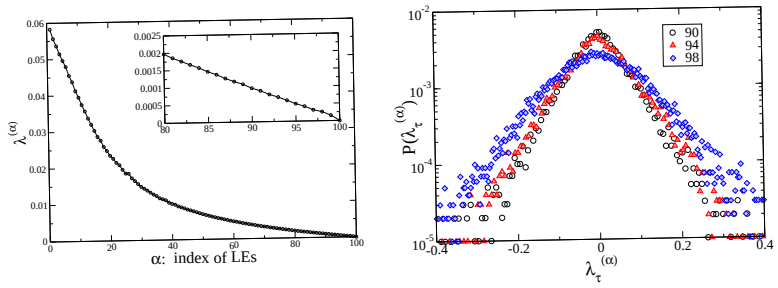

Figure 1. Left: Lyapunov spectrum. Right: Distribution of the finite-time Lyapunov exponent $\lambda_\tau^{(\alpha)}$ where τ is equal to the period of re-orthonormalization.

The fluctuations in local instabilities of trajectories is demonstrated by means of the distribution of finite-time LEs. By definition, finite-time Lyapunov exponents λ_τ measure the expansion rate of trajectory segments of the duration τ. In Fig. 1, such distributions are presented for some LEs in the regime $\lambda \approx 0$. Fluctuations of the finite time Lyapunov exponents are quite large compared to the difference between their mean values, i.e., $\sigma(\lambda_\tau^{(\alpha)}) \equiv \sqrt{\langle {\lambda_\tau^{(\alpha)}}^2 \rangle - \langle \lambda_\tau^{(\alpha)} \rangle^2} \gg |\lambda^{(\alpha)} - \lambda^{(\alpha+1)}|$. Here, $\langle \cdots \rangle$ means time average. The strong fluctuations in local instabilities constitute one of the possible reasons for the disappearance of the step-wise structures in the Lyapunov spectra. They could also cause the mixing of nearby Lyapunov vectors. The mixing may be at the basis of the intermittency observed in the time evolution of the spatial Fourier transformation of LVs (see Sect. 4.2.1).

4.2.1 Intermittency in Time Evolution of Instantaneous Static LV Structure Factors

Based on the spatial Fourier transformation of $u^{(\alpha)}(x,t)$

$$\tilde{u}_k^{(\alpha)}(t) = \int u^{(\alpha)}(x,t) \exp(-ikx) dx = \sum_{j=1}^{N} \delta x_j^{(\alpha)} \cdot \exp[-ik \cdot x_j(t)] \tag{5}$$

we introduce a quantity called *instantaneous static LV structure factor*, which reads

$$s_{uu}^{(\alpha)}(k,t) \equiv |\tilde{u}_k^{(\alpha)}(t)|^2. \tag{6}$$

It is nothing but the instantaneous spatial power spectrum of $u^{(\alpha)}(x,t)$.

The time evolution of the instantaneous static LV structure factor $s_{uu}^{(95)}(k,t)$ for Lyapunov vector No. 95 is shown in Fig. 2 as an example. Two quantities are recorded as time goes on. One is the peak wave-number k_*, which marks the position of the highest peak in the spectrum $s_{uu}^{(\alpha)}(k,t)$ (see Fig. 2). The other is the spectral entropy $H_s(t)$, which measures the distribution property of the spectrum $s_{uu}^{(\alpha)}(k,t)$. It is defined as:

$$H_s(t) = -\sum_{k_i} s_{uu}^{(\alpha)}(k_i,t) \ln s_{uu}^{(\alpha)}(k_i,t). \tag{7}$$

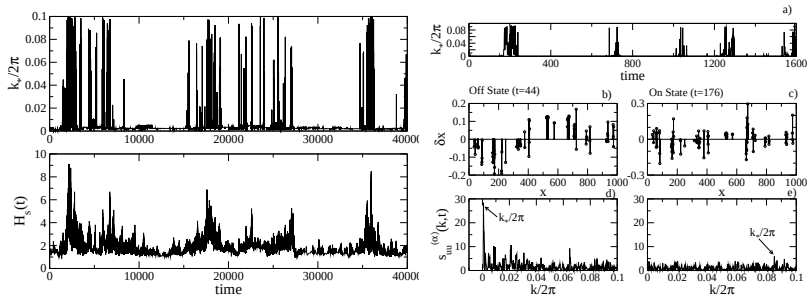

Figure 2. Left: Intermittent behaviours of the peak wave-number k_* and spectral entropy $H_s(t)$ for the spatial Fourier spectrum of $u^{(95)}(x,t)$. Right: a) Variation of the peak wave number k_* with time. b),c) Two typical snapshots of LV_{95}, *off* and *on* state at $t = 44$ and 176 respectively. d),e) their spatial Fourier transform.

A smaller value of $H_s(t)$ means that the spectrum $s_{uu}^{(\alpha)}(k,t)$ is highly concentrated on a few values of k, i.e., these components dominate the behaviour of the LV. Both of these quantities behave intermittently, as shown in Fig. 2. Large intervals of nearly constant low values (*off state*) are interrupted by short period of bursts (*on state*) where they have large values. Details of typical *on* and *off* states are shown in the right part of Fig. 2. One can see that the off state is dominated by low wave-number components (see the sharp peak at low wave-number k_*), while the on state is more noisy and there are no significant dominant components. This intermittency in the time evolution of the instantaneous static LV structure factors is a typical feature of soft potential systems. It is conjectured that this is a consequence of the mixing of nearby LVs caused by the wild fluctuations of local instabilities. Due to the mutual interaction among modes, the hydrodynamic Lyapunov modes in the soft potential systems are only of finite life-time. In the dynamic Lyapunov structure function estimated, the peak representing the propagating (or oscillating) Lyapunov modes is of finite width. This is support for our conjecture that the hydrodynamic Lyapunov modes are of finite life-time.

4.2.2 Dispersion Relation of Hydrodynamic Lyapunov Modes

Now, we consider the static LV structure factor $S_{uu}^{(\alpha)}(k)$, which is the long-time average of the instantaneous quantity $s_{uu}^{(\alpha)}(k)$. Two cases with $L = 1000$ and 2000 are shown in Fig. 3. It is not hard to recognize the sharp peak at $\lambda \approx 0$ in the contour plot of the spectrum. With increasing Lyapunov exponents, the peak shifts to the larger wave number side. A dashed line is plotted to make clear how the wave number of the peak k_{max} changes with $\lambda^{(\alpha)}$.

All of our results shown above provide strong evidence of the fact that the Lyapunov vectors corresponding to the smallest positive LEs in our 1d Lennard-Jones system are highly dominated by a few components with small wave numbers, i.e, they are similar to the Hydrodynamic Lyapunov modes found in hard-core systems. The wave-like character becomes weaker and weaker as the value of the LE is increased gradually from zero.

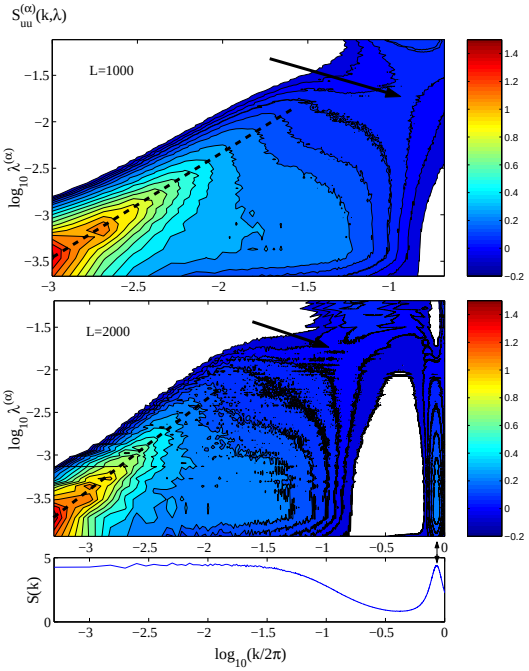

Figure 3. Contour plot of the spectra $S_{uu}^{(\alpha)}(k)$ for $L = 1000$ and 2000. A ridge structure can easily be recognized in the regime $k \approx 0$ and $\lambda \approx 0$. To guide the eyes, a dashed line is plotted to show how the peak wave-number k_{max} changes with λ.

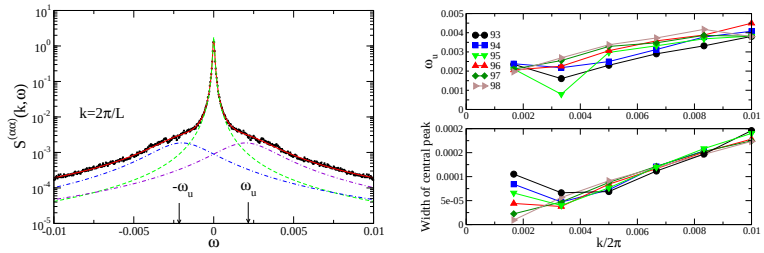

Figure 4. Left: Dynamic LV structure factor $S_u^{(\alpha\alpha)}(k,\omega)$ for $\alpha = 96$ and $k = 2\pi/L$. The full line results from a 3-pole fit. The corresponding decomposition into three Lorentzians is also shown. Right: Dispersion relations $\omega^{(\alpha)}(k)$ (top) and the $k-$dependence of the width of the central peak (bottom) obtained from 3-pole approximations.

4.3 Dynamic LV Structure Factors

More detailed information about the dynamical evolution of Lyapunov vectors can be obtained from the dynamic LV structure factors $S_u^{(\alpha\alpha)}(k,\omega)$, which encode in addition to the structural also the temporal correlations. In Fig. 4 we show a typical example for

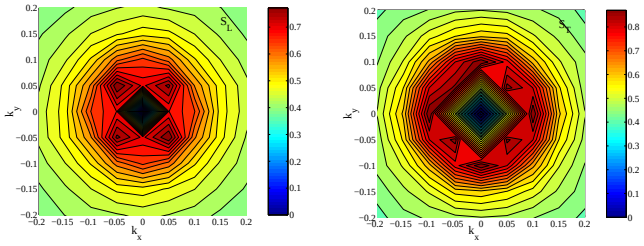

Figure 5. Contour plots of $S_L^{(\alpha\alpha)}(\vec{k})$ and $S_T^{(\alpha\alpha)}(\vec{k})$ of a LV with $\alpha = 140$ in a $2d$ system with $N = 100$, $T = 0.8$ and $L_x \times L_y = 20 \times 20$. Obviously, the longitudinal and transverse components behave differently.

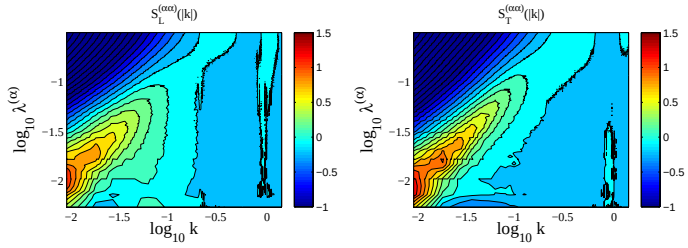

Figure 6. Contour plots of $S_L^{(\alpha\alpha)}(k)$ and $S_T^{(\alpha\alpha)}(k)$ (left) and the corresponding dispersion relation $\lambda(k)$ (right) of the hydrodynamic Lyapunov modes in a $2d$ system with $N = 100$, $T = 0.8$ and $L_x \times L_y = 5 \times 120$.

$S_u^{(\alpha\alpha)}(k,\omega)$. It consist of a central "quasi-elastic" peak with shoulders resulting from dynamical excitations quite similar to the dynamic structure factor $S(k,\omega)$ of fluids[16]. In order to extract the dynamical information we use a 3-pole approximation for $S_u^{(\alpha\alpha)}(k,\omega)$, which amounts to fitting the latter by a superposition of three Lorentzians, one central peak at $\omega = 0$ and two symmetric peaks located at $\omega = \pm\omega_u(k)$. The fits are also shown in the figure. They describe the frequency dependence of $S_u^{(\alpha\alpha)}(k,\omega)$ quite well. These fits allow us to extract the dispersion relations $\omega^{(\alpha)}(k)$ for each of the hydrodynamic Lyapunov modes with index α. The results are shown in Fig. 4 for several of the Lyapunov modes. Clearly, this tells us that a Lyapunov mode corresponding to exponent λ is characterized, apart from the dominating wave number $k(\lambda)$, by a typical frequency $\omega(k(\lambda))$. Because $\frac{d\omega}{dk}$ is non-vanishing, this implies propagating wave-like excitations. The full LV dynamics of the soft-potential system treated here, however, is more complex than that of the hard-core systems. For instance, the peaks in $S_u^{(\alpha\alpha)}(k,\omega)$ are of finite width (see Fig. 4). This fact is consistent with our observation that several quantities characterizing the dynamical aspect of Lyapunov vectors evolve erratically in time (see Sec. 4.2.1).

5 Lyapunov Modes in 2d Lennard-Jones Fluids

In isotropic fluids with $d > 1$ the static LV structure factor $S_u^{(\alpha\alpha)}(\vec{k})$ becomes a second rank tensor. Cartesian components $S_{\mu\nu}^{(\alpha\alpha)}(\vec{k})$ of $S_u^{(\alpha\alpha)}(\vec{k})$ can be expressed in terms

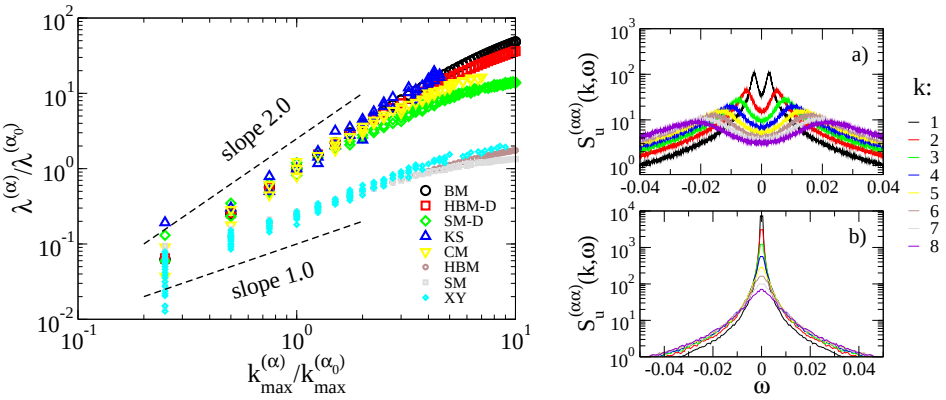

Figure 7. Left: The λ-k dispersion relations for various extended systems with continuous symmetries. The normalized data for different systems collapse on two master curves. These results strongly support our conjecture that there are two classes of systems with $\lambda \sim k$ and $\lambda \sim k^2$ respectively. Systems in the group with $\lambda \sim k$ include Eq.(8) with $f(z) = \frac{1}{2\pi}\sin(2\pi z)$ (SM), Eq.(8) with $f(z) = 2z \pmod 1$ (HBM) and the 1d XY model (XY). Systems belonging to class $\lambda \sim k^2$ are Eq.(10) with $f(z) = \frac{1}{2\pi}\sin(2\pi z)$ (CM), Eq.(10) with $f(z) = 2z \pmod 1$ (BM), Eq.(8) with $f(z) = \frac{1}{2\pi}\sin(2\pi z)$ and $\gamma = 0.7$ (SM-D), Eq.(8) with $f(z) = 2z \pmod 1$ and $\gamma = 0.7$ (HBM-D) and the 1d Kuramoto-Sivashinsky equation (KS). Right: Dynamic LV structure factors $S_u^{(\alpha\alpha)}(k,\omega)$ for a) coupled standard maps, Eq.(8) with $\epsilon = 1.3$; b) coupled circle maps, Eq.(10) with $\epsilon = 1.3$.

of longitudinal and transverse correlation functions $S_L^{(\alpha\alpha)}$ and $S_T^{(\alpha\alpha)}$ as $S_{\mu\nu}^{(\alpha\alpha)}(\vec{k}) = \hat{k}_\mu\hat{k}_\nu S_L^{(\alpha\alpha)}(k) + (\delta_{\mu\nu} - \hat{k}_\mu\hat{k}_\nu)S_T^{(\alpha\alpha)}(k)$ with $\hat{k}_\mu = (\vec{k}/k)_\mu$. As an example, we presented in Fig. 5 the contour plot of the two correlation functions S_L and S_T for LV No. 140 of a two-dimensional Lennard-Jones system with $N = 100$, $T = 0.8$ and $L_x \times L_y = 20 \times 20$. The difference between the two components is quite obvious. However, as can be seen from Fig. 6, $S_L^{(\alpha\alpha)}(k)$ and $S_T^{(\alpha\alpha)}(k)$ for two-dimensional cases behave similar to the one-dimensional case shown in Fig. 3. This fact implies the existence of hydrodynamic Lyapunov modes also in two-dimensional cases. In addition, both the longitudinal and transverse components are characterized by a linear dispersion relation, which has been found to be typical of Hamiltonian systems[12,13]. Further numerical simulations show that the transverse modes are non-propagating , in contrast to the longitudinal components.

6 Universal Features of Lyapunov Modes in Spatially Extended Systems with Continuous Symmetries

Relying on the LV correlation function method, we have up to now successfully identified the existence of HLMs in the following spatially extended systems:
Coupled map lattices (CMLs) with either Hamiltonian or dissipative local dynamics

$$v_{t+1}^l = (1-\gamma)v_t^l + \epsilon[f(u_t^{l+1} - u_t^l) - f(u_t^l - u_t^{l-1})] \tag{8}$$

$$u_{t+1}^l = u_t^l + v_{t+1}^l \tag{9}$$

and

$$u_{t+1}^l = u_t^l + \epsilon[f(u_t^{l+1} - u_t^l) - f(u_t^l - u_t^{l-1})]. \tag{10}$$

Dynamic XY model with the Hamiltonian

$$H = \sum_i \dot{\theta}_i + \epsilon \sum_{ij} [1 - cos(\theta_j - \theta_i)]. \tag{11}$$

Kuramoto-Sivashinsky equation

$$h_t = -h_{xx} - h_{xxxx} - h_x^2. \tag{12}$$

A common feature of these systems is that they all hold certain continuous symmetries and conserved quantities, which have been shown to be essential for the occurrence of Lyapunov modes[12]. Our numerical simulations and analytical calculations indicate that these systems fall into two groups with respect to the nature of hydrodynamic Lyapunov modes. To be precise, the dispersion relations are characterized by $\lambda \sim k$ and $\lambda \sim k^2$ in Hamiltonian and dissipative systems respectively, as Fig. 7 indicates. Moreover, the HLMs in Hamiltonian systems are propagating, whereas those in dissipative systems show only diffusive motion. Examples of dynamic LV structure factors for two CMLs are presented in the right row of Fig. 7. In a), each spectrum has two sharp symmetric side-peaks located at $\pm\omega_u$. Furthermore, $\omega_u \simeq \pm c_u k$ for $k \geq 2\pi/L$. These facts suggest that the HLMs in coupled standard maps are propagating. The spectrum of coupled circle maps in b) has only a single central peak and can be well approximated by a Lorentzian curve[12], which implies that the HLMs in this system fluctuate diffusively. In addition, no step structures in Lyapunov spectra have been found in contrast to the hard-core systems. The quantities characterizing the dynamical evolutions of LVs in these systems exhibit intermittent behaviour.

7 Conclusion and Discussion

We have presented numerical results for the Lyapunov instability of Lennard-Jones systems. Our simulations show that the step-wise structures found in the Lyapunov spectrum of hard-core systems disappear completely here. This is presumed to be the result of the strong fluctuations in the finite-time LEs[3]. A new technique based on the spatial Fourier spectral analysis is employed to reveal the vague long wave-length structure hidden in LVs. In the resulting spatial Fourier spectrum of LVs with $\lambda \simeq 0$, a significantly sharp peak with low wave-number is found. This serves a strong evidence of the existence of hydrodynamic Lyapunov modes in soft-potential systems[18]. The disappearance of the step-structures and the survival of the hydrodynamic Lyapunov modes show that the latter are more robust and essential than the former. Studies on dynamical LV structure factors provide evidence that longitudinal HLMs in Lennard-Jones fluids are propagating. Going beyond many-particle systems, we have shown that, for a large class of extended systems, HLMs of Hamiltonian and dissipative cases are different both in respect of spatial structure and in the dynamical evolution.

Acknowledgments

We thank W. Just, W. Kob, A. Latz, A. S. Pikovsky and H. A. Posch for fruitful discussions. Special thanks go to W. Kob for providing us with the code of molecular dynamics simulations and to G. Rünger and M. Schwind for the help on the parallel algorithms. We acknowledge financial support from the DFG within SFB393 "Parallele Numerische Simulation für Physik und Kontinuumsmechanik" and Ra416/6-1 and a grant of computer time provided by the John von Neumann Institute for Computing.

References

1. J.P. Dorfman, *An Introduction to Chaos in Nonequilibrium Statistical Mechanics*. Cambridge University Press, Cambridge (1999).
2. H.A. Posch and R. Hirschl, *Simulation of billards and of hard-body fluids*. In: Szasz, D. (ed) Hard Ball Systems and the Lorenz Gas. Springer, Berlin (2000).
3. C. Forster, R. Hirschl, H.A. Posch and Wm.G. Hoover, Physics D, **187**, 294-310 (2004).
4. J.-P. Eckmann and O. Gat, J. Stat. Phys., **98**, 775-798 (2000).
5. S. McNamara and M. Mareschal, Phys. Rev. E, **64**, 051103 (2001).
6. A. de Wijn and H. van Beijeren, Phys. Rev. E, **70**, 016207 (2004).
7. T. Taniguchi and G.P. Morriss, Phys. Rev. E, **65**, 056202 (2002); Phys. Rev. E, **68**, 026218 (2003).
8. Wm.G. Hoover, H.A. Posch, C. Forster, C. Dellago and M. Zhou, J. Stat. Phys., **109**, 765-776 (2002).
9. H.-L. Yang and G. Radons, Phys. Rev. E, **71**, 036211 (2005), see also arXiv:nlin.CD/0404027.
10. G. Radons and H.-L. Yang, arXiv:nlin.CD/0404028.
11. H.-L. Yang and G. Radons, Phys. Rev. Lett. **96**, 074101 (2006).
12. H.-L. Yang and G. Radons, Phys. Rev. E **73**, 016202 (2006).
13. H.-L. Yang and G. Radons, Phys. Rev. E **73**, 016208 (2006).
14. G. Benettin, L. Galgani and J.M. Strelcyn, Phys. Rev. A, **14**, 2338-2345, (1976); I. Shimada and T. Nagashima, Prog. Theor. Phys., **61**, 1605-1616 (1979).
15. G. Radons, G. Rünger, M. Schwind, and H.-L Yang, In J. Dongarra, K. Madsen, and J. Wasniewski (eds.): Applied Parallel Computing, Proceedings of PARA04, Lyngby, June 20-23, 2004, Lecture Notes of Computer Science **3732**, pp. 1131, Springer, Berlin (2006).
16. J.P. Boon and S. Yip, *Molecular Hydrodynamics*. McGraw-Hill, New York (1980).
17. J.-P. Eckmann, C. Forster, H.A. Posch and E. Zabey, J. Stat. Phys., **118**, 795-811 (2005).
18. C. Forster and H.A. Posch, New J. Phys., **7**, 32 (2005), see also arXiv:nlin.CD/0409019.